A Study on the Autoignition Characteristics of the Pre-mixture of DME/LPG in a HCCI Engine

Thongchai Sakda[1], Jamsran Naranhuu[1], Park Kyuyeol[2], Lee Youngjae[3], Lim Ocktaeck[*2]

[1] Graduate of Mechanical Engineering, Ulsan University, Mugeo-dong, Nam-gu, Ulsan 680-749, Korea
[2] School of Mechanical Engineering, University of Ulsan, San 29, Ulsan 680-749, Korea,
[3] Korea Institute of Energy Research, 102 Gajeong-ro, Yuseong-gu, Daejeon 305-343, Korea
*Corresponding Author: otlim@ulsan.ac.kr, Tel: +82-52-259-2852, Fax: +82-52-259-1680

Abstract

This study was investigated to examine the potential increase of engine power through the mixture of DME and LPG on HCCI combustion. The effects of mixing ratio of DME/LPG in constant intake temperature were confirmed experimentally in a single cylinder diesel engine. A numerical analysis were conducted through the mixing model of DME and n-Butane for the detailed chemical kinetics using CHEMKIN-PRO to clarify the autoignition mechanism of constant combustion phasing. The results show that the increased amount of LPG reduces the LTHR and activates the HTHR which increases the in-cylinder pressure. Therefore, it has potential to raise the IMEP by appropriately changing the mixing ratio. Also, thermal efficiency was increased to 51.2% at the mixing ratio of 0.6. Finally, engine out emissions including THC and CO were decreased by the change of mixing ratio. Numerical results agreed with experiment that the weakened low temperature oxidation by the increase of n-Butane amount.

Keywords*:* Mixing ratio, DME, n-Butane, Combustion phase, HCCI

1. Introduction

The homogeneous charge compression ignition (HCCI) engine is named as the candidate of next generation internal combustion engine with the high efficiency of the CI engine and the very low emissions of the SI engine. The known benefits of a HCCI engine are near-zero nitrogen oxides (NOx) and PM emissions. However, several items have to solve before its widespread production. Controlling the rate of energy release and pressure-rise at high loads have been main problems [1]. There are many attempts made to overcome the problem of early ignition timing, which are making heterogeneous mixture or thermal stratification [2-5], adding cooled EGR [6], and mixing two different characteristics of fuels as high cetane and high octane number fuels [7], or vice versa. Among them, fuel selections for large reactivity difference fuels have been one of the important aspects of HCCI engine development. Adjusting the appropriate proportions of high cetane number fuel and high octane number fuel may control the ignition timing and expand the operation range of HCCI combustion. To approach that way, dimethyl ether (DME) and liquefied petroleum gas (LPG) were used in this study as a fuel. DME has been taking much attraction as known the alternative of diesel fuel

with smokeless combustion, low ignition temperature, superior properties of evaporation and available to produce from wide ranges of sources as natural gas, coal and vegetarian, etc. Besides these good characteristics, early ignition and short burn duration have been main obstacle and limits the wide production of DME fueled vehicles or the other applications [8-11]. On the other hand, LPG has similar characteristics with DME while it has 40% higher value of lower heating than that of DME. Therefore, adding LPG into DME as ignition inhibitor is the promising technology [12-14]. Since normal butane is main component of LPG, authors have conducted a modeling work on DME/n-Butane pre-mixture which shows that optimized mixing ratio has the potential to delay autoignition timing by reducing pressure rise rate (PRR). This is a continued work to get better understanding in the aspect of fundamentals for reaction mechanism since ignition of HCCI takes place by the dominance of chemical kinetics. The main objective of this study is to computationally investigate the autoignition mechanism of the DME/n-Butane mixture in case of chemical kinetics. The “Contribution matrix to heat release” and “Absolute heat-release rate” of important elementary reactions are used for each fuel to identify the underlying mechanism by varying the mixing ratios.

2. Methods

2.1 Experimental setup

Fig. 1 shows a schematic of engine which is a single cylinder diesel engine with a displacement of 498 cc. The engine specifications are showed in Table 1. From the left side of the schematic, intake system, engine and exhaust system are shown. Air was supplied from the intake system with naturally aspirated and metered by the air flow meter. Fuel was injected from the distance of 800mm of the intake valve. The reason for the distance from the intake valve was to maximize the pre-mixture of fuel and air. The temperatures for pre-mixture and exhaust gas were measured by the temperature sensors which were installed at intake valve and exhaust valve, respectively. The in-cylinder pressure was measured by the pressure sensor which was located at the center of the cylinder head.

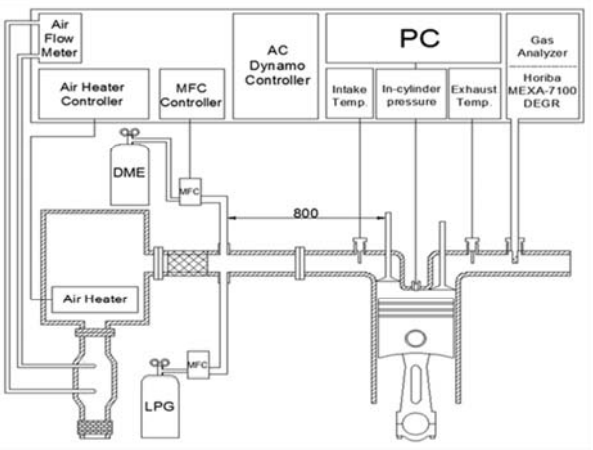

Fig. 1 Schematic of the engine facility.

Table. 1 Engine specifications.

	Experiment	Calculation
Process	4 stroke	Only one comp. /expansion
Number of cylinders	1	-
Displaced volume	498 cc	498 cc
Stroke	92 mm	92 mm
Bore	83 mm	83 mm
Connecting Rod	145.8 mm	145.8 mm
Compression ratio	19.5:1	19.5:1
Number of Valves	2	2
Inlet Valve Close	136° bTDC	136° bTDC
Exhaust Valve Open	125.4° aTDC	125.4° aTDC
Fueling system	Fully premixed	Fully premixed

2.2 Operation conditions

DME and LPG were used as a fuel by injecting into the intake manifold to make the pre-mixture. DME was the main fuel. Dual fuel's mixing ratio was defined by the following equation and mixing ratios as well equivalence ratios regarding to the mixing ratio of each fuel are shown in Table 2.

$$\text{Mixing ratio of DME, } X_{DME}\ [-] = \frac{\text{DME(g/cycle)}}{\text{DME(g/cycle)} + \text{LPG(g/cycle)}} \quad (1)$$

Table. 2 Mixing ratio definition and equivalence ratio.

Mixing ratio of DME, X_{DME} [-]	DME [%]	LPG [%]	φ_{DME} [-]	$\varphi_{n\text{-Butane}}$ [-]
1.0	100	0	0.57	0.00
0.9	90	10	0.51	0.06
0.8	80	20	0.45	0.12
0.7	70	30	0.39	0.18
0.6	60	40	0.34	0.23
0.5	50	50	0.28	0.29
0.4	40	60	0.22	0.35
0.3	30	70	0.17	0.40
0.2	20	80	0.11	0.46
0.1	10	90	0.05	0.52
0.0	0	100	0.00	0.57

2.3 Computational Approach

2.3.1 Chemical-kinetics modeling setup

The computational investigations were conducted using the single-zone model of CHEMKIN included in CHEMKIN-PRO [15]. The single-zone model treats the in-cylinder charge as a single lumped mass with uniform composition and thermodynamic properties. Heat-transfer and blow-by effects were not included. Compression / expansion was modeled according to the standard slider-crank relationship [16], using the geometry and specifications of the single-cylinder HCCI engine as shown in Table 1. The calculation starts from the intake valve close (IVC) of 136° bTDC to the exhaust valve open (EVO) of 125.4° aTDC. The single-zone model allows relatively short computational times even with the detailed chemical-kinetic mechanisms, so numerous changes in operation conditions can be readily examined. In this modeling work, the ratio of DME and n-Butane was defined by the following equation.

$$X_{DME} = \frac{n_{DME}}{n_{DME} + n_{n-Butane}} \quad (2)$$

n_{DME}: Mole number of DME during 1 cycle [mol/cycle]

$n_{n-Butane}$: Mole number of n-Butane during 1 cycle [mol/cycle]

Chemical kinetic scheme for the mixture of two fuels with 185 species and 730 reactions was created through the models from Curran's di-methyl ether (DME) [17-18] and Kojima's n-Butane [19] whose chemical kinetics mechanisms and thermodynamic parameters were used. Therefore, the validation of this new mixing model was conducted using shocktube calculation and the results shown in Fig. 2 for the ignition delay as a function of intake-temperature in case of mixture ratio.

Solid lines are results of the mixing model while circle and rectangular points are the data from original models of DME and n-Butane. As can be seen in the figure, ignition delay of the mixture increases as the amount of n-Butane under 1100K is increased due to the long ignition delay characteristics of n-Butane at lower

temperature. However, the ignition delay timing was nearly similar at higher intake temperatures between 1100 K and 1600 K. In general, because of the near similarity of experimental data of DME and n-Butane for the temperature range, mixing model was thought to be utilized for further calculation through its validation with experimental data [17-19]. Properties of these fuels are showed in Table 3.

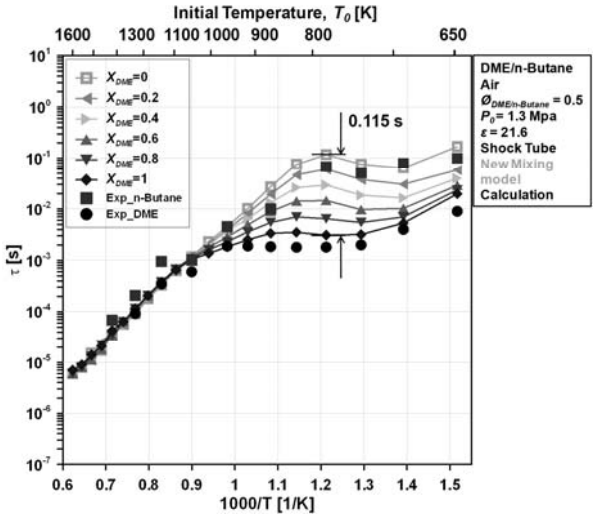

Fig. 2 Shock-Tube results for variation of DME ratios vs. experimental ignition delays (points) for DME [17-18] and n-Butane [19].

Table 3. Fuel properties

Items	DME	n-Butane	Diesel	Gasoline
Molecular Formula	CH_3OCH_3	C4H10	-	-
Low Heat Value [MJ/kg]	28.8	45.8	42.7	43.2
Cetane Number	55-60	<10	40-55	13-17
LTHR / Total HR *100 [%]	10~30	0~5	-	-
HTHR / Total HR *100 [%]	70~90	95~100	-	-

DME fuel is considered a promising clean alternative fuel for ground transportation vehicles, and it can be substitute for conventional diesel fuel in a compression ignition diesel engine [11]. n-Butane has low cetane number characteristics and is not able to ignite itself as DME. Molecular ratio of air was as follows N2:O2:Ar = 78:21:1. For this modeling study, no attempt is made to capture the effect of trace hydrocarbon species such as carbon monoxide (CO), hydrocarbons (HC) and partially-oxidized hydrocarbons encountered experimentally in real EGR. The beginning of the main heat release marks the onset of hot chemistry with breaks down of H2O2 at temperature around 1100K. Refer to the maximum temperature, the onset of misfire reactions can be judged when reaching the temperature below 1100K [20]. Reactions involved dominantly in the autoignition of DME and n-Butane were divided in three main groups which are fuel series reactions, H2O2 loop reactions and hydrogen-oxygen (H2O2) system reactions, which are illustrated in Fig. 3.

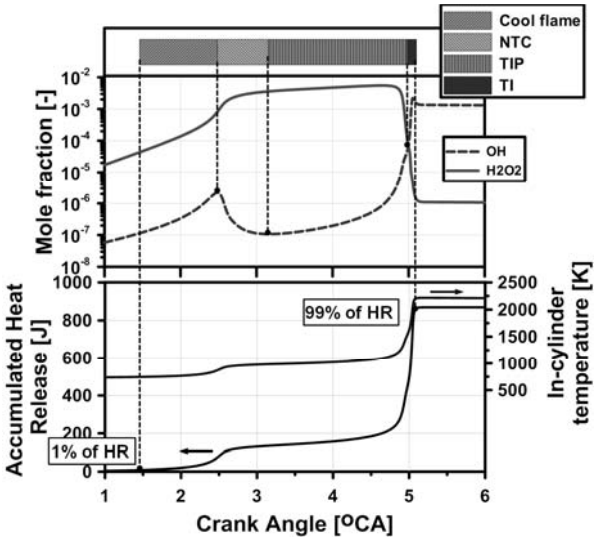

Fig. 3 Definition of key combustion timings.

2.3.2 Contribution matrix to heat release

The autoignition process can be simplified by the extracting important reactions from detailed chemical kinetics mechanisms using “contribution matrix to heat release” [21] as shown in Eq.3.

$$CHR_{j,Tt} = \frac{HR_{j,Tt}}{\sum_{j=1}^{N} abs(HR_{j,Tt})} \cdot 100\% \quad (3)$$

Here, $CHR_{j,Tt}$ is the contribution ratio of jth elementary reaction to heat release at a transient temperature T_t. $HR_{j,Tt}$ is the heat release rate by the j^{th} elementary reaction at T_t. This study utilized the data for the value of contribution ratio to heat release of important elementary reactions above 3% at T_t.

3. Results

3.1 Effects of mixing ratio on combustion phasing

Fig. 4 shows the combustion characteristics for the change of mixing ratio of DME and LPG at same input calorific value.

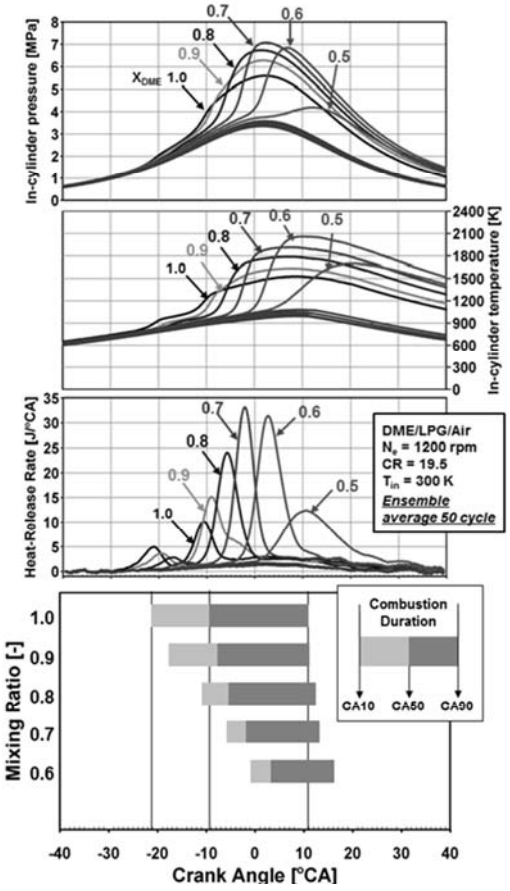

Fig. 4 In-cylinder pressure, temperature, heat release and combustion duration as a function of mixing ratio.

In-cylinder pressure was increased till mixing ratio of 0.7 but decreased when mixing ratio was less than 0.6. The peak pressure was abruptly reduced as 4.19MPa from X_{DME}=0.5 and the amount of heat release was also decreased. From less than 0.4 of mixing ratio, the in-cylinder temperature was lower than 1100K. It can be seen that combustion phasing has been retarded by the LPG content and duration was reduced due to higher energy density of LPG in the mixture. Fig. 5 shows the IMEP and thermal efficiency for the various mixing ratio. COV of IMEP took its peak at X_{DME} =0.5 as 42% while its normal value should be within 8% [22-23].

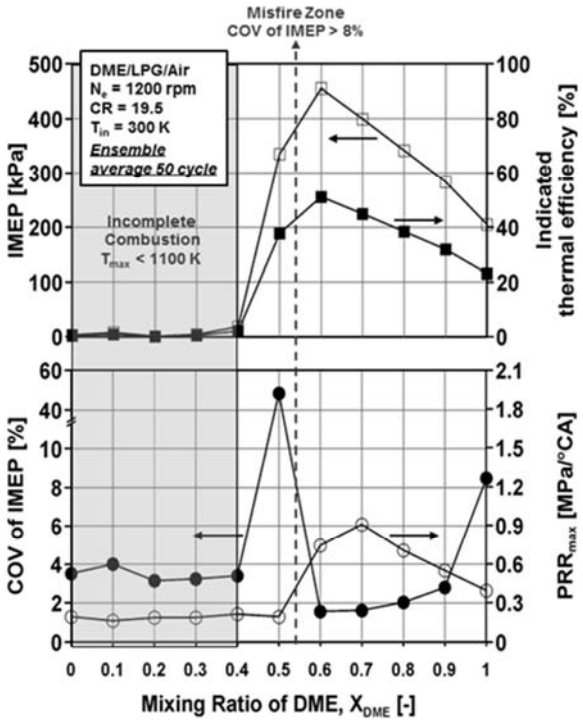

Fig. 5 IMEP, indicated thermal efficiency, COV of IMEP and maximum pressure rise rate for the mixing ratio of DME.

As mentioned before, the ratios are lower than 0.5 results in the misfire operation. Therefore, IMEP was the highest at 0.6 for considering above conditions, where IMEP and thermal

efficiency were increased by 250kPa and 28.2%, respectively, compared to X_{DME}=1.0. The combustion process takes place around the beginning of expansion stroke for the highest IMEP condition as X_{DME}=0.6. Therefore, the low temperature heat release (LTHR) was decreased while the high temperature heat release (HTHR) was increased for the change of mixing ratio. From the data-set for emissions in Fig. 6, the amount of THC and CO was decreased at the combustion zone where the in-cylinder temperature was higher than 1500K.

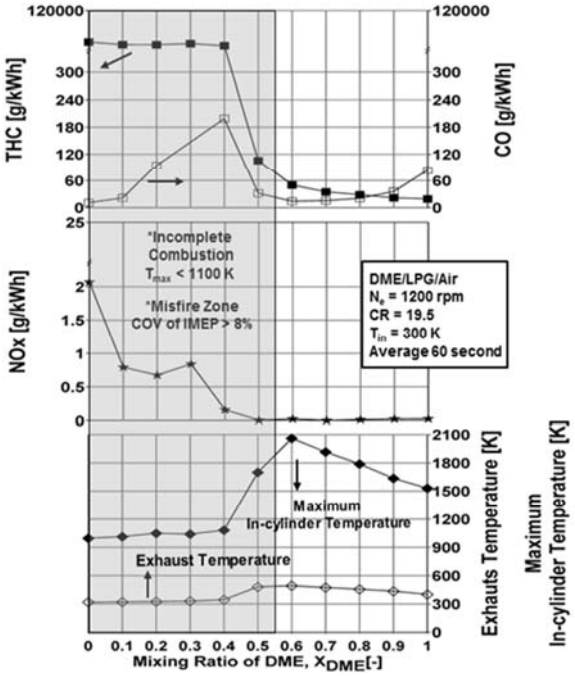

Fig. 6 THC, CO, NOx emissions, exhaust gas temperature and maximum in-cylinder temperature as a function of mixing ratio of DME for same operating condition shown in Fig. 5.

NOx emissions were resulted very low since the in-cylinder temperature was lower than 2200K for all the cases of combustion zone. Typically, HC and CO were generated when the in-cylinder temperature was lower than 1500K due to the no decomposition process from H2O2 to OH at lean and cold side of the cylinder [24-25].

3.2 Modeling results for the mixing ratio

Fig. 7 shows the comparison of modeling results for simulation with experiment. To match the results from the modeling to experiment, the compression ratio was adjusted by reducing to 15 since there was no heat transfer effect in the modeling. In order to obtain the fundamental knowledge about the autoignition process of the two fuels of mixture, chemical kinetic modeling study was exercised.

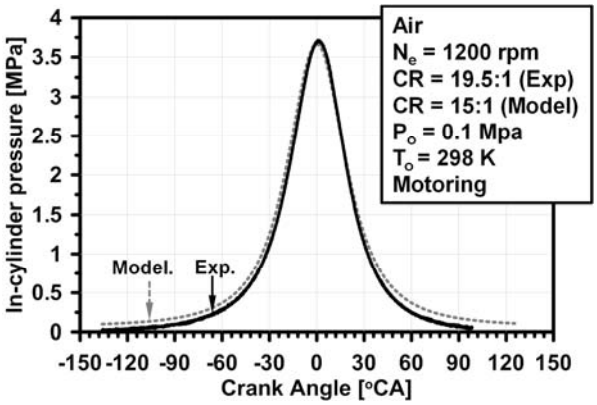

Fig. 7 Comparison of in-cylinder pressure traces of motoring for the model and experiment.

The supplied fuel/ air equivalence ratio was 0.57 and intake caloric value was 770 J/cycle throughout the change of mixing ratio to maintain the effect of fuel. Also, the mole number was fixed by the value of the base point which was selected for X_{DME}=1.0, 300K and 0.1MPa. Therefore, the mole number and intake calorific value were fixed constant by adjusting the intake pressure and temperature with the change of mixing ratio. Fig. 8 shows how the intake pressure and temperature must be changed to obtain above mentioned baseline point and

combustion duration and key combustion temperatures were shown.

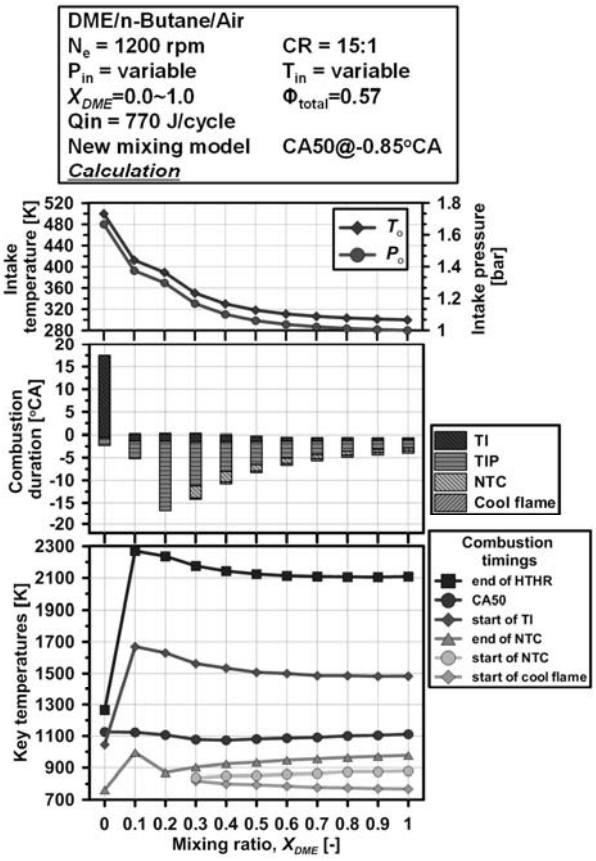

Fig. 8 Effect of mixing ratio on required intake temperature, combustion duration and key combustion temperatures in constant phasing operation.

As the reduce of n-Butane amount in the mixture, both intake temperature and pressure dramatically reduced. The lower cetane number of n-Butane shows the slow autoignition reactivity. The combustion duration was increased by the lengthen of TIP as the increase of n-Butane amount in the mixture. There was single stage combustion occurred as the mixture ratio increased over 0.3, where the combustion duration was the longest. The combustion temperatures were reduced at DME side since its intake pressure and temperatures were lower than that of n-Butane side. Cool flame start temperature was increased but other temperatures were decreased at n-Butane side. Fig. 9 shows PRR, RI and IMEP as a function of mixing ratio for the data plotted in Fig. 8. PRR and RI were gradually increased as the increase of n-Butane from 0.4.

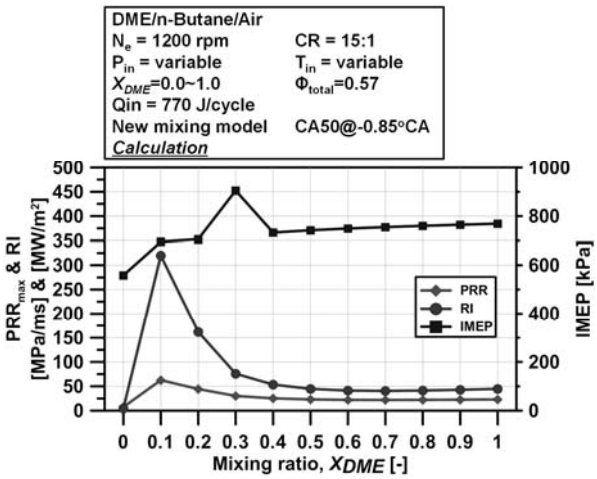

Fig. 9 Effect of mixing ratio of DME on PRR, ringing intensity (RI) [3] and IMEP for the data plotted in Fig. 8.

IMEP resulted the identical amount and no such big difference between the mixing ratios. Therefore, in Fig. 9, mixing ratio 0.5 and 1.0 were compared to confirm the influences on autoignition and how it differs during the combustion process in view point of chemical kinetics. Although the effects of the mixing ratio were briefly explained above, its mechanism on autoignition is still unclear. What factor is influenced on the increase of combustion duration by reduced combustion temperature? In order to clarify the underlying mechanism and answer the question, the heat release of elementary reactions involved in the autoignition were separately considered with autoignition regimes.

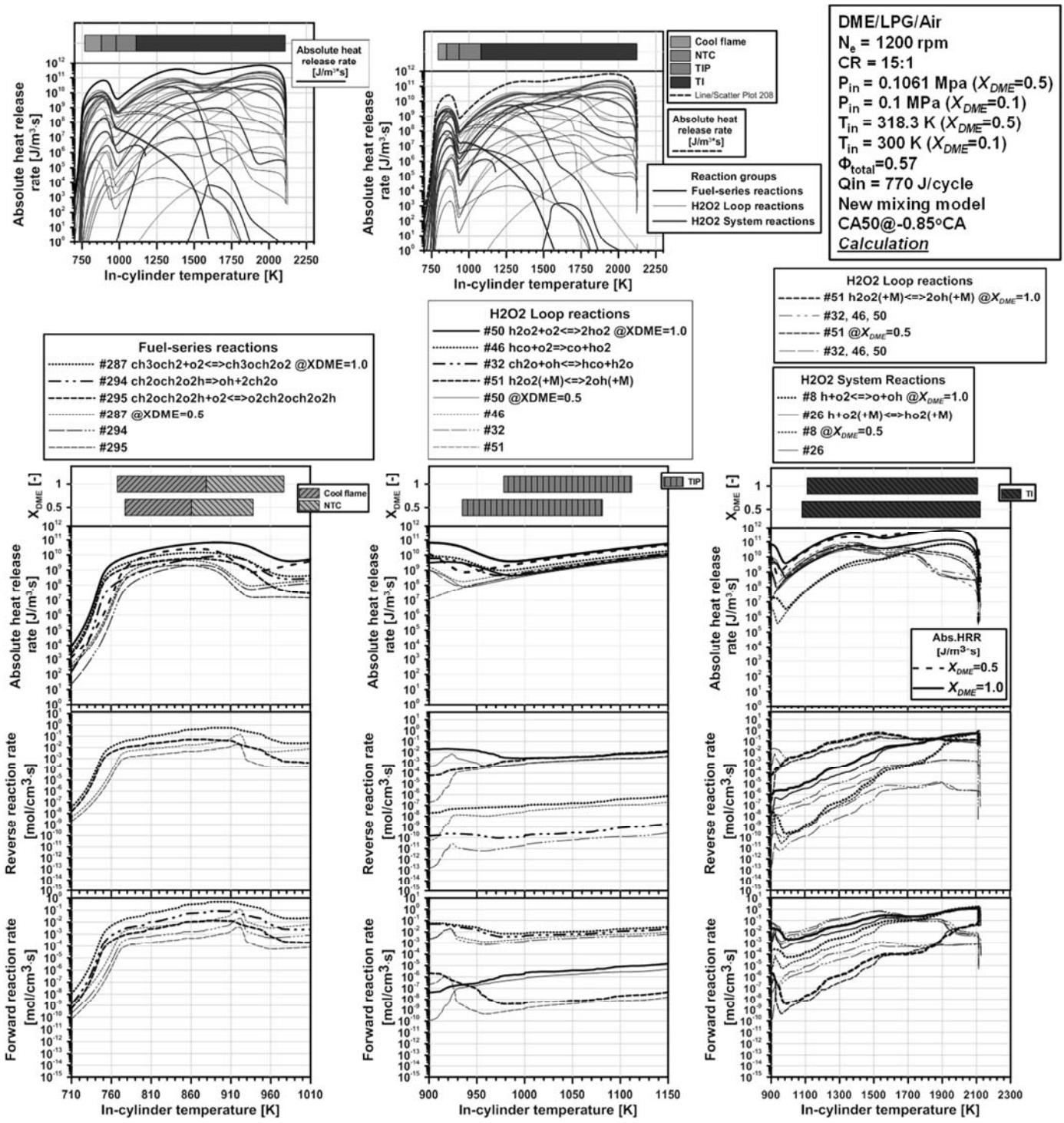

Fig. 10 Absolute HRR and reaction rates for dominant reactions in autoignition of DME/n-Butane HCCI combustion in case of XDME=0.5 and 1.0

.

Therefore, contribution matrix to heat release in which reactions were above the threshold as 3% was utilized and it gives the possibility to distinguish the important reactions participated in autoignition process of DME/n-Butane HCCI combustion. As can be seen in the Fig. 10, absolute heat release for overall dominant reactions and rates of those reactions in separate autoignition regimes for X_{DME}=0.5 and 1.0 were selected for the comparison.

As can be seen from the legend at the top left side of the figure, absolute HRR is black line, which was higher abs.HRR and longer temperature duration at X_{DME}=1.0 compared to 0.5. To better understand these phenomena, the elementary reactions were divided into three main groups as fuel-series, H2O2 loop, and H2O2 system reactions [22].

Cool-flame and NTC range: Among the fuel-series reactions, primary O2 addition by 287 reaction and secondary O2 addition by 295 reaction are dominant in cool flame. Reaction 294 is transition reaction from cool-flame to NTC which suppresses the reaction rate. The equilibrium of these reactions shift toward the reactants side and the addition of O2 to the alkyl radical is almost completely extinguished with the higher temperatures. The temperature range for cool flame surrounded between 770K and 880K for X_{DME}=1.0 while it was started at 780K and transmitted at 860K to NTC range for 0.5. It was thought that the existence of n-Butane shortens the temperature range of cool flame. In case of NTC, it was terminated at 980K and 924K for the cases, respectively. The lower transition temperature of cool flame to NTC was a reason for longer duration of NTC in Fig. 8. In order to comprehend the underlying mechanism of this event, reaction rates of both reverse and forward were plotted along with the in-cylinder temperature for autoignition ranges. Reactions go follow a similar trend to absolute HRR within these regions. Absolute HRR of primary O2 addition reaction (287) was higher at X_{DME}=1.0 than that of 0.5 case. Around 860K for 0.5, decomposition reaction (294) was crossed with secondary O2 addition reaction (295) and went upward since its forward reaction rate was increased, which was taken place around 870K for X_{DME}=1.0. Therefore, HRR for the reaction (294) was responsible for the occurrence of NTC, which was solely increased at the transition region of NTC from cool flame. In both cases, reverse reaction of 294 was not taken place. During the NTC range, rates of all reactions were decreased and terminated at 980K and 920K for both cases. Mainly this trend was comparable with combustion duration. In both cases, the minimum transient temperature of reaction 294 for HRR after the first peak was matched up to the end of NTC.

Thermal-ignition preparation and thermal ignition: The role of TIP reactions is to increase the temperature to initiate the TI. After the fuel series reactions, H2O2 loop reactions were the main contributor to TI range in TIP range, which plays an important role in the thermal ignition by supplying heat rather than radicals. During the NTC range, almost reactions rates and heat release decreased but the only reaction was increased without falling down along with the increase of the in-cylinder temperature which was H2O2 decomposition reaction (51) to generate OH. TIP begins around 980K and 925K after NTC in both cases. At X_{DME}=0.5, NTC was terminated at lower temperature and TIP was started and went through the lower reaction rates, in which forward reaction rates were decreased as the in-cylinder temperature is increased. This is the reason of slowed down of autoignition with lower heat release and longer burn duration at TIP range. It can be also confirmed in combustion duration in Fig. 7, where TIP was lengthened evidently at X_{DME}=0.5. In TI range, although there

are a number of reactions contributed as plotted in the absolute heat release graph on top of figure, hydrogen-oxygen system reaction was initiated by the decomposition of H2O2 and the increase of OH, in which the competition of branching chain reaction (8) and HO2 recombination reaction (26) are dominant along with temperature. As the temperature increase after TIP, reaction (51) of H2O2 loop was also contributor to take place of thermal ignition among the other reactions, of which reaction rates are higher than other reactions of loop. Reverse reaction rates of X_{DME}=0.5 were higher than that of X_{DME}=1.0 case, while it was inverse at forward reaction rate. This higher reverse reaction rate of H2O2 loop reactions at X_{DME}=0.5 case might be responsible for evidently longer TIP duration. At X_{DME}=0.5, combustion temperature was lower and duration of TI was longer even CA50 was identical with X_{DME}=1.0. At forward reaction rate of X_{DME}=0.5, the competition of reaction (8) and (26) was not strong and it terminates at lower temperature. It was thought that the reason of increased duration of TI along with crank angle.

4. Conclusions

In this work, we attempted to increase the engine output by mixing of DME and n-Butane. Based on the experimental results, numerical work was conducted to understand the autoignition process in view point of chemical kinetics. From this study, the following conclusions can be drawn:

1) IMEP was increased slightly when X_{DME} was changed from 1.0 to 0.6 and took the peak value (455kPa) at mixing ratio of 0.6 due to the higher energy content of n-Butane compared to pure DME.

2) Thermal efficiency was similar trend with IMEP and had the maximum value at 0.6 as 51.2%.

3) The minimum values for THC and CO belonged to the mixing ratio of DME at 1.0 and 0.6 respectively. THC and CO were simultaneously reduced when X_{DME} was 0.8. NOx almost does not exist.

New mixing model of DME and n-Butane mixture was validated successfully and followed the data under the condition of experimental study. Low temperature oxidation reactions were weakened with increased n-Butane content and decreased the temperature of high temperature oxidation. However, reaction paths of the HTO were identical during the temperature from 1000 to 2100K.

5. Acknowledgments

This research was financially supported by the Ministry of Education (MOE) and National Research Foundation of Korea (NRF) through the Human Resource Training Project for Regional Innovation and Basic Science Research Program through the National Research Foundation of Korea (NRF) funded by the Ministry of Education, Science and Technology (2012R1A1A1044855).

6. References

[1] F. Zhao, T.W. Asmus, D.N. Assanis, J.E. Dec, J.A. Eng, P.M. Najt (Eds.), *Homogeneous charge compression ignition (HCCI) engines: Key Research and Development Issues*, Society of Automotive Engineers, Warrendale, PA, 2003.

[2] Y. Yang, J.E. Dec, N. Dronniou, M. Sjöberg, Tailoring HCCI heat-release rates with

partial fuel stratification: Comparison of two-stage and single-stage-ignition fuels, Proc. Combust. Inst. 33 (2011) 3047-3055.

[3] D. Yang, Z. Wang, J. Wang, S. Shuai, Experimental study of fuel stratification for HCCI high load extension, Appl Energy, 88 (9) (2011) 2949-2954.

[4] H. Zhang, E.R. Hawkes, J.H. Chen, S. Kook, A numerical study of the autoignition of dimethyl ether with temperature inhomogeneities, Proc. Combust. Inst. 34 (2013) 803-812.

[5] B. Peterson, E. Baum, B. Böhm, V. Sick, A. Dreizler, High-speed PIV and LIF imaging of temperature stratification in an internal combustion engine, Proc. Combust. Inst. 34 (2013) 3653-3660.

[6] M. Sjöberg, J.E. Dec, Effects of EGR and its constituents on HCCI autoignition of ethanol, Proc. Combust. Inst. 33 (2011) 3031-3038.

[7] S. Shi, Recent progress in combustion technologies for automotive engines, J Combust Sci Technol, 7 (2001) 1-15.

[8] DME Handbook, Japan DME forum, Ohmsha Ltd, Japan, 2007.

[9] T.A. Semelsberger, R.L. Borup, H.L. Greene, Dimethyl ether (DME) as an alternative fuel, Journal of Power Sources. 156 (2006) 497-511.

[10] C. Arcoumanis, C. Bae, R. Crookes, E. Kinoshita, The potential of di-methyl ether (DME) as an alternative fuel for compression-ignition engines: A review, Fuel 87 (2008) 1014-1030.

[11] S. Park, C. Lee, Combustion performance and emission reduction characteristics of automotive DME engine system. Prog. Energy Combust. Sci. 39 (2013) 147-168.

[12] C. Oh, J. Jang, C. Bae, The effect of LPG composition on combustion and performance in a DME-LPG dual-fuel HCCI engine, SAE paper 2010-01-0336, 2010.

[13] X. Lu, D. Han, Z. Huang, Fuel design and management for the control of advanced compression-ignition combustion modes, Prog. Energy Combust. Sci. 37 (2011) 741-783.

[14] S. Lee, S. Oh, Y. Choi, K. Kang, Effect of n-Butane and propane on performance and emission characteristics of an SI engine operated with DME-blended LPG fuel, Fuel. 90 (2011) 1674-1680.

[15] CHEMKIN-PRO 15131, Reaction Design, San Diego, CA (2013).

[16] J.B. Heywood, Internal Combustion Engine Fundamentals, McGraw-Hill, New York (1988).

[17] S.L. Fischer, F.L. Dryer, H.J. Curran, The reaction kinetics of dimethyl ether. I: high-temperature pyrolysis and oxidation in flow reactors, Int. J. Chem. Kinet. 32 (2000) 713–740.

[18] H.J Curran, S.L. Fischer, F.L. Dryer, The reaction kinetics of dimethyl ether. II: low-temperature pyrolysis and oxidation in flow reactors, Int. J. Chem. Kinet. 32 (2000) 741–759.

[19] S. Kojima, Detailed modeling of n-Butane autoignition chemistry, Combust. Flame 99 (1994) 87-136.

[20] S. Park, C. Lee, Combustion performance and emission reduction characteristics of automotive DME engine system, Prog. Energy Combust. Sci. 39 (1) (2013) 147-168.

[21] H. Yamada, H. Sakanashi, N. Choi, A. Tezaki, Simplified oxidation mechanism of DME applicable for compression ignition, SAE paper 2003-01-1819, 2003.

[22] H. Ando, Y. Sakai, K. Kuwahara, Universal rule of hydrocarbon oxidation, SAE Paper 2009-01-0948, 2009.

[23] Y. Nakamura, D.W. Jung, N. Iida, Closed-loop combustion control of a HCCI engine with re-breathing EGR system, SAE paper 2013-32-9069, 2013.